JOURNAL OF GUIDANCE, CONTROL, AND DYNAMICS
Vol. 18, No. 5, September–October 1995

Feedback Linearization Autopilot Design for the Advanced Kinetic Energy Missile Boost Phase

Harvey J. Gratt*
KBM Enterprises, Inc., Huntsville, Alabama 35803
and
Wayne L. McCowan†
U.S. Army Missile Command, Redstone Arsenal, Alabama 35898

This paper describes an application of feedback linearization to the design of an autopilot for the boost phase of the advanced kinetic energy missile, a hypervelocity missile being developed by the U.S. Army Missile Command. The rapid change in missile states during the boost phase, coupled with a requirement for accurate guidance, provide a challenge for the autopilot designer. Application of the feedback linearization methodology permitted an autopilot design to be successfully accomplished without the necessity for generating numerous airframe transfer functions and frozen-point stability plots. The resulting autopilot is easily updated to accommodate changes in the missile design.

Nomenclature

C_M = aerodynamic moment coefficient
$C_{M\alpha}$ = partial derivative of the moment coefficient C_M due to α
C_N = normal force coefficient
$C_{N\alpha}$ = partial derivative of the normal force coefficient C_N due to α
d = reference diameter
I = moment of inertia
M = missile mass
M_α = $(QSd/I)C_{M\alpha}$
M_δ = $(QSd/I)C_{M\delta}$
N_α = $(QS/MV)C_{N\alpha}$
N_δ = $(QS/MV)C_{N\delta}$
Q = dynamic pressure, $0.5\rho V^2$
q = airframe pitch rotation rate
S = reference area
T = thrust
V = missile velocity
XCG = distance from missile nose to center of gravity
XCP = distance from missile nose to center of pressure
α = pitch plane angle of attack
$\dot{\gamma}$ = flight-path angle rate in pitch plane
δ = control surface deflection
η = lateral acceleration
θ = pitch-attitude angle
$\dot{\theta}$ = pitch-attitude rate
$\hat{}$ = estimated parameter

Introduction

THE tactical version of the advanced kinetic energy missile (ADKEM) is vertically launched, carries a kinetic energy penetrator, and is designed for use against both ground and airborne targets. The missile centerbody carries the flight computer, the inertial instruments, the control actuation system, and the penetrator rod. Although an early concept for the tactical missile envisioned use of strapdown inertial navigation for boost phase guidance, for early flight testing the only inertial sensors utilized onboard were three rate gyros.

After being popped-up out of the launch canister, the missile is oriented toward the target by a discardable thrust vector control package prior to ignition of the four strap-on boost motors. The strap-on boosters burn for less than half a second after ignition and during this time propel the missile to a velocity greater than Mach 6. This is the boost phase referred to in this paper. During this boost phase, control force for stabilization and guidance is supplied by movement of the rear control fins in the boost motor plumes. Full control force is, thus, available immediately after booster ignition.

This paper presents the results of an application of feedback linearization[1–3] to the design of an autopilot for the ADKEM boost phase.[4] This technique provides an autopilot design methodology which solves problems resulting from the almost linear (in the boost phase), but highly time varying nature of this missile, although preserving the usefulness of point stability techniques. The resulting gamma-dot ($\dot{\gamma}$) autopilot was developed without the requirement for the tedious and time consuming process of generating numerous airframe transfer functions and frozen-point stability plots to develop gains for gain scheduling. The design methodology also allows updates to the autopilot to be made rapidly, even with major changes to the system. Prior to the first test flight, the thrust time history for the boosters, which had been built for the test flight, was found to differ in both magnitude and duration from those of all of the prior motors (baseline design) that had been built and tested and on which the autopilot design was based. The autopilot updates were completed within 1 h after receipt of the new thrust data.

In addition to the large variations in the aerodynamic, mass, and inertia properties of the ADKEM missile that occur during the boost phase (Mach 0 to greater than Mach 6 in less than 0.5 s), several constraints were faced by the autopilot designers. In the airframe design, the inertial sensor package on the missile was located aft of the missile center of gravity, and this placement could not be changed. The maximum control force available was limited by the root bending moment structural limitations of the control fin actuators. Although wind-tunnel tests were conducted to estimate airframe aerodynamic characteristics, the location of the airframe center of pressure (hence, the static margin) in the Mach number range associated with the last-half of the boost phase had an uncertainty (not a known variation) of up to ±2 calibers.

Feedback Linearization

A relatively recent development in the design and analysis of nonlinear systems is the concept of feedback linearization (sometimes called dynamic inversion).[1–3] As will be subsequently shown,

Presented as Paper 93-3736 at the AIAA Guidance, Navigation, and Control Conference, Monterey, CA, Aug. 9–11, 1993; received March 7, 1994; revision received Dec. 19, 1994; accepted for publication Dec. 22, 1994.

*Manager, Guidance and Control, 15980 Chaney Thompson Road.
†Aerospace Engineer Researcher, Guidance and Control Analysis Branch, Research, Development, and Engineering Center. Member AIAA.

the concept is easily extended to time varying systems. In feedback linearization, a state variable transformation is performed on a nonlinear system model such that the resulting transformed system is represented by a simpler, linear, time-invariant model to which linear design techniques can be applied.[5–9] The technique is best introduced by way of example. Assume a nonlinear system described by the state equations

$$\dot{X}_1 = a(\sin X_2) \tag{1a}$$

$$\dot{X}_2 = -X_1^2 + U \tag{1b}$$

If it is desired to control the X_1 variable, one may proceed as follows: Let

$$Z_1 = X_1 \tag{2a}$$

$$Z_2 = \dot{Z}_1 = \dot{X}_1 = a(\sin X_2) \tag{2b}$$

Differentiating Z_2 until a term involving the control appears results in

$$\dot{Z}_2 = \ddot{X}_2 = a(\cos X_2)\left(-X_1^2 + U\right) \equiv V \tag{2c}$$

where V is the new system control variable. The transformed system is, thus, given by

$$\dot{Z}_1 = Z_2 \tag{3a}$$

$$\dot{Z}_2 = V \tag{3b}$$

which is a linear, time-invariant system, and V can be designed as desired. For instance, if a proportional plus integral (PPI) controller is required, define

$$V = A\int (V_c - Z_1)\,\mathrm{d}t - BZ_1 - CZ_2 \tag{4}$$

and Eqs. (3) can be expressed as

$$\dot{Z}_1 = Z_2 \tag{5a}$$

$$\dot{Z}_2 = A\int (V_c - Z_1)\,\mathrm{d}t - BZ_1 - CZ_2 \tag{5b}$$

Laplace transforming Eqs. 5 and applying Cramer's rule results in

$$\frac{Z_1}{V_c} = \frac{X_1}{X_{1c}} = \frac{A}{s^3 + Cs^2 + Bs + A} \tag{6}$$

where A, B, and C are desired polynomial coefficients. Equation (6) represents a linear, time-invariant system from X_{1c} to the desired output X_1. The control may now be expressed in terms of the original system states and control variable. From Eq. (2c) one has

$$U = \frac{V}{a(\cos X_2)} + X_1^2 \tag{7}$$

or, substituting from (4)

$$U = \left\{\left[A\int (X_{1c} - X_1)\,\mathrm{d}t - BX_1 - Ca(\sin X_2)\right]\Big/ a(\cos X_2)\right\} + X_1^2 \tag{8}$$

Advanced Kinetic Energy Missile Gamma-Dot Autopilot

It was decided to implement a gamma-dot (velocity vector turn rate) autopilot for the ADKEM application for a number of reasons: 1) it provides explicit control of the missile velocity vector turn rate; 2) it is essentially a type 1 acceleration design; 3) it requires no precompensator to obtain the proper steady-state value; and 4) the only sensor outputs required for implementation are body rotational rates, which avoids problems associated with having accelerometers (aft of the missile center of gravity) in the autopilot feedback on a tail controlled airframe.

An estimator structure is used to reconstruct the missile pitch and yaw plane gamma-dots. The use of rate sensors only does introduce an error in estimating the gamma dots if the estimated missile N_α is in error. The tradeoff, however, becomes that of stability vs estimator (and thus performance) degradation. Six-degree-of-freedom (DOF) simulation results indicated that the stability issue was significant but that the estimator error issue was tolerable. Thus, the use of rate sensors only (no accelerometers) for autopilot stabilization feedback appeared to be a feasible implementation.

The application of feedback linearization to the ADKEM autopilot design will now be described. Only the pitch channel will be shown since the pitch and yaw channels are essentially identical other than for sign differences. The design is obtained using a simplified airframe model, which retains the detail required for a useful solution. Linear, time-invariant methods applied to the transformed system model will be used to account for the effects of sampling, gyro and actuator dynamics, and flexible body bending. The missile equations of motion are not recapitulated herein; see Ref. 10.

Proceeding, let

$$X_1 = \left(N_\alpha - \frac{N_\delta M_\alpha}{M_\delta} + \frac{T}{MV}\right)\alpha = N'_\alpha \alpha = \dot{\gamma} \tag{9}$$

$$X_2 = q \tag{10}$$

$$\dot{\alpha} = q - \dot{\gamma} \tag{11}$$

(In the autopilot, $\dot{\gamma}$ will be estimated and this estimate will be the controlled variable.) Differentiating Eqs. (9) and (10) yields the two state equations

$$\dot{X}_1 = N'_\alpha(q - N'_\alpha\alpha) + \dot{N}'_\alpha\alpha \tag{12}$$

$$\dot{X}_2 = M_\alpha\alpha + M_\delta\delta \tag{13}$$

Defining a state coordinate transformation by

$$Z_1 = X_1 \tag{14}$$

$$Z_2 = \dot{X}_1 \tag{15}$$

yields the transformed system

$$\dot{Z}_1 = Z_2 \tag{16}$$

$$\dot{Z}_2 = N'_\alpha[M_\alpha\alpha + M_\delta\delta - N'_\alpha(q - N'_\alpha\alpha) - \dot{N}'_\alpha\alpha] + 2\dot{N}'_\alpha(q - N'_\alpha\alpha) + \ddot{N}'_\alpha\alpha \equiv V \tag{17}$$

i.e.,

$$\begin{aligned}\dot{Z}_1 &= Z_2\\ \dot{Z}_2 &= V\end{aligned} \tag{18}$$

which is a (transformed) linear, time-invariant system.

To provide a type-1 gamma-dot autopilot, V is chosen as

$$V = C_0\left[\tau(V_c - Z_1) + \int (V_c - Z_1)\,\mathrm{d}t\right] - C_2 Z_2 - C_1 Z_1 \tag{19}$$

where [from Eqs. (14) and (9)]

$$Z_1 \equiv \dot{\gamma} \tag{20}$$

$$V_c \equiv \dot{\gamma}_c \tag{21}$$

Equations (16) and (17) can be solved for Z_1 as

$$\frac{Z_1}{V_c} = \frac{C_0(\tau s + 1)}{s^3 + C_2 s^2 + (C_1 + \tau C_0)s + C_0} = \frac{C_0(\tau s + 1)}{s^3 + C_2 s^2 + C'_1 s + C_0} \tag{22}$$

Equations (16) and (17) can also be solved for δ in terms of all pertinent quantities as

$$\delta = \frac{1}{N'_\alpha M_\alpha}\left\{C_0\left[\int (V_c - \dot{\gamma})\,\mathrm{d}t + \tau(V_c - \dot{\gamma})\right] - C_2[N'_\alpha(q - N'_\alpha\alpha) + \dot{N}'_\alpha\alpha] - (C'_1 - \tau C_0)N'_\alpha\alpha - N'_\alpha M_\alpha\alpha + \left(N'^2_\alpha - 2\dot{N}'_\alpha\right)(q - N'_\alpha\alpha) + N'_\alpha\dot{N}'_\alpha\alpha - \ddot{N}'_\alpha\alpha\right\} \tag{23}$$

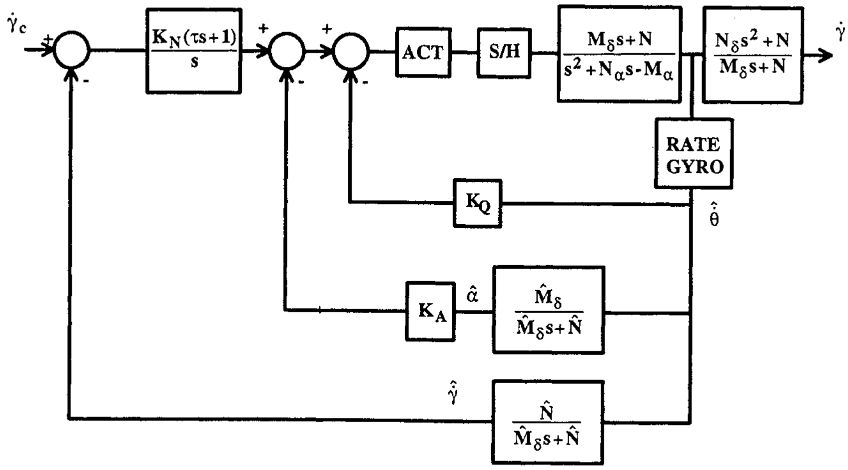

Fig. 1 Pitch and yaw gamma-dot autopilot, boost phase.

If all of the time-varying terms are lumped into a correction term, denoted by CR, where

$$CR = -\frac{\alpha}{N'_\alpha M_\delta}[\dot{N}'_\alpha - \dot{N}'_\alpha(C_2 + 3N'_\alpha)] - \frac{2\dot{N}'_\alpha q}{N'_\alpha M_\delta} \tag{24}$$

then Eq. (23) reduces to

$$\delta = \frac{K_N(\tau s+1)}{s}(V_c - \dot{\gamma}) - K_Q q - K_A\alpha + (CR) \tag{25}$$

with

$$K_N = C_0/N'_\alpha M_\delta = C_0/N \tag{26}$$

$$K_Q = (C_2 - N'_\alpha)/M_\delta \tag{27}$$

$$K_A = (C'_1 + M_\alpha - K_Q N - K_N \tau N)/M_\delta \tag{28}$$

These are the nominal time-invariant type-1 $\dot{\gamma}$-autopilot gain definitions with C_0, C'_1, and C_2 defining the placement of the closed-loop poles. The autopilot can, thus, be designed in a conventional manner, and the appropriate correction signals (CR) can be injected as required.

Autopilot Loop Analysis

To analyze the resulting autopilot design (point stability), a worst-case loop analysis was performed using the following procedure.

1) Set $\dot{\gamma}_c$ to zero.

2) Break the loop ahead of the actuator and obtain the open-loop (OL) transfer function (Fig. 1).

In the resulting expression, the actuator (act), gyro dynamics, sample and hold (S/H), and compensation delay (comp) appear in series as

$$\mathrm{OL} = [\mathrm{S/H} + \mathrm{comp}][\mathrm{act} + \mathrm{gyro}]\left[\frac{M_\delta s + N}{s^2 + N_\alpha s - M_\alpha}\right] \times \left[K_Q + \frac{K_A M_\delta}{M_\delta s + N} + \frac{K_N(\tau s+1)N}{s(M_\delta s + N)}\right] \tag{29}$$

Recall that

$$N \equiv M_\delta N_\alpha - N_\delta M_\alpha = M_\delta N'_\alpha \tag{30}$$

which, when substituted into Eq. (29), results in

$$\mathrm{OL} = [\mathrm{S/H} + \mathrm{comp}][\mathrm{act} + \mathrm{gyro}]\left[\frac{M_\delta s + N}{s^2 + N_\alpha s - M_\alpha}\right] \times \left\{K_Q M_\delta\left[s^2 + \left(\frac{K_A}{K_Q} + N'_\alpha + \frac{K_N \tau N'_\alpha}{K_Q}\right)s + \frac{K_N}{K_Q}N'_\alpha\right] \Big/ s(M_\delta s + N)\right\} \tag{31}$$

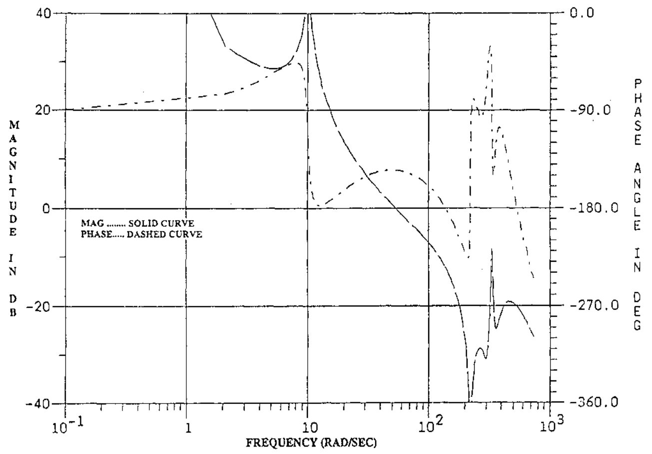

Fig. 2 Coast phase gamma-dot autopilot open-loop frequency response, no latency effects.

From Eqs. (26) and (27), it can be seen that

$$\frac{K_N}{K_Q} = \frac{C_0}{K_Q N} = \frac{C_0}{(C_2 - N'_\alpha)N'_\alpha} \tag{32}$$

and from Eqs. (28) and (30), that one has

$$K_A = (1/M_\delta)[C'_1 + M_\alpha - K_Q M_\delta N'_\alpha - K_N M_\delta N'_\alpha \tau] \tag{33}$$

The coefficient of the s term in the numerator of Eq. (31) can be expressed, using Eqs. (26–28), (32), and (33) in the form

$$\frac{K_A}{K_Q} + N'_\alpha + \frac{K_N \tau N'_\alpha}{K_Q} = \frac{C'_1 + M_\alpha}{C_2 - N'_\alpha} \tag{34}$$

For the s^0 coefficient, simplification yields

$$K_N N'_\alpha / K_Q = C_0/(C_2 - N'_\alpha) \tag{35}$$

Substituting Eqs. (34) and (35) into (31) results in

$$\mathrm{OL} = [\mathrm{S/H} + \mathrm{comp}][\mathrm{act} + \mathrm{gyro}] \times \left[\frac{M_\delta s + N}{s^2 + N_\alpha s - M_\alpha}\right]\left[(C_2 - N'_\alpha)\left\{s^2 + \left(\frac{C'_1 + M_\alpha}{C_2 - N'_\alpha}\right)s + \frac{C_0}{C_2 - N'_\alpha}\right\} \Big/ s(M_\delta s + N)\right] \tag{36}$$

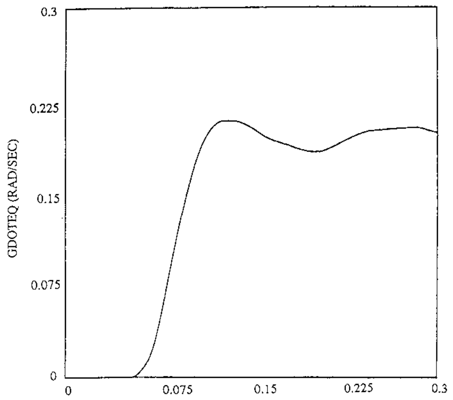

Fig. 3 Gamma-dot autopilot step response, boost phase.

or, denoting estimated aero with a caret,

$$\mathrm{OL} = [\mathrm{S/H} + \mathrm{comp}][\mathrm{act} + \mathrm{gyro}]\left[\frac{M_\delta s + N}{s^2 + N_\alpha s - M_\alpha}\right]$$
$$\times\left[(C_2 - \hat{N}'_\alpha)s^2 + (C'_1 + \hat{M}_\alpha)s + C_0\big/s(\hat{M}_\delta s + \hat{N})\right] \tag{37}$$

If structural modes are to be included, the airframe transfer function block is replaced by

$$\left[\frac{M_\delta s + N}{s^2 + N_\alpha s - M_\alpha} + \text{flex mode transfer function}\right] \tag{38}$$

Linear Analysis

Applying a conventional frequency domain analysis to the boost autopilot allows a quick iteration to the final design, thus, for the pitch and yaw autopilot channels: real pole at 10 rps, $\tau = 0.1$; quadratic pole at 50, 0.7 damped; provisions for a double notch structural filter; inner-loop compensations to provide phase compensation for S/H and actuator lags; phase margin $\approx$27 deg; gain margin $\approx$9 dB (defined at a representative point during boost). Figure 2 depicts a Bode plot for this configuration. Figure 3 illustrates the autopilot response to a step command of 0.2 rad/s input at 0.05 s into boost.

Conclusions

Feedback linearization has been shown to be a viable approach for the analysis and synthesis of an autopilot for a missile system of this type, which must function in a regime involving very high (greater than 1000 g) axial acceleration and rapid variation in plant parameters.

Appendix: Three-Loop Conventional Acceleration Autopilot

It is of interest to analyze and evaluate the performance of the well-known three-loop autopilot[11] configuration depicted in Fig. A1 as applied to the ADKEM boost-phase mission. This was the first autopilot configuration examined for application to this missile. Applying the following synthesis procedure utilizing feedback linearization to this configuration will yield a desired configuration similar to that of the $\dot{\gamma}$ autopilot, specifically the use of angle-of-attack feedback in lieu of $\int \dot{\theta}\, dt$ for the middle loop as well as the loops incorporating $\dot{N}_\alpha$ and $\ddot{N}_\alpha$ terms. Poor transient response was obtained from the three-loop configuration during the early boost phase, and it is conjectured that this was a direct consequence of the $\int \dot{\theta}\, dt$ feedback loop. Furthermore, results from high-fidelity 6-DOF digital simulations have shown that for the ADKEM boost phase the conventional three-loop configuration yields catastrophically poor performance if α feedback is not used.

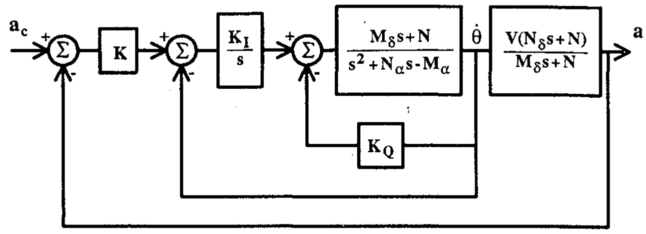

Fig. A1 Conventional acceleration autopilot.

First, consider the normal point stability approach applied to the system shown in Fig. A1. For the ensuing discussions we neglect fin (N_δ), actuator, and gyro dynamics. The inclusion of fin dynamics can be trivially handled via block diagram manipulation of the appropriate numerator dynamics and can also be incorporated into the state space based approach utilized by the feedback linearization method. For simplicity, these added manipulations are not performed since they are not germane to the key results.

Under these assumptions, the following output transfer function is derived from Fig. A1:

$$\frac{a}{a_c} = \frac{KK_I V_M N}{s^3 - (N_\alpha + K_q M_\delta)s^2 + (-M_\alpha + K_q N + K_I M_\delta)s + (K_I N + KK_I V_M N)} = \frac{A}{s^3 + Ds^2 + Es + (C + A)} \tag{A1}$$

The normal design procedure is to assume A, C, E, and D are constant values from a desired polynomial and solve for the gains K, K_q, and K_I. At this point, note that the sum $A + C$ is considered to be a constant in order to obtain a consistent set of equations. This procedure yields the pole-placement design associated with the three-loop autopilot. The resulting design is then assumed extendable to the case of time varying aerodynamic parameters.

Equating the denominators in Eq. (A1) yields

$$K_q = (D - N_\alpha)/M_\delta \tag{A2}$$

$$K_I = (E + M_\alpha - K_q N)/M_\delta \tag{A3}$$

$$K = [(A + C) - K_I N]/K_I V_M N \tag{A4}$$

This autopilot configuration results in a steady-state gain $\neq$1, thus, some form of pregain may be required.

Now consider the same three-loop configuration in the context of the plant model given by

$$a = -V_M N'_\alpha \alpha \equiv Z'_\alpha \alpha$$
$$\dot{q} = M_\alpha \alpha + M_\delta \delta \tag{A5}$$

where a is lateral acceleration. Also note that

$$\dot{\gamma} = N'_\alpha \alpha \tag{A6}$$

$$Z'_\alpha M_\delta = -V_M N'_\alpha M_\delta = -VN \tag{A7}$$

Defining $X_1 = a$, $X_2 = q$, then

$$\dot{X}_1 = \dot{Z}'_\alpha \alpha + Z'_\alpha \dot{\alpha} \tag{A8}$$

$$\dot{X}_2 = M_\alpha \alpha + M_\delta \delta \tag{A9}$$

$$\dot{\alpha} = q - \dot{\gamma} = q + (a/V_M) \tag{A10}$$

These equations form the basic state space description of the airframe.

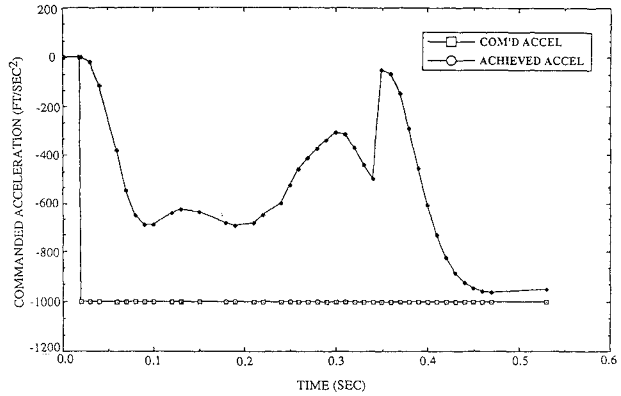

Fig. A2 Commanded and achieved lateral acceleration, without time-varying correction terms.

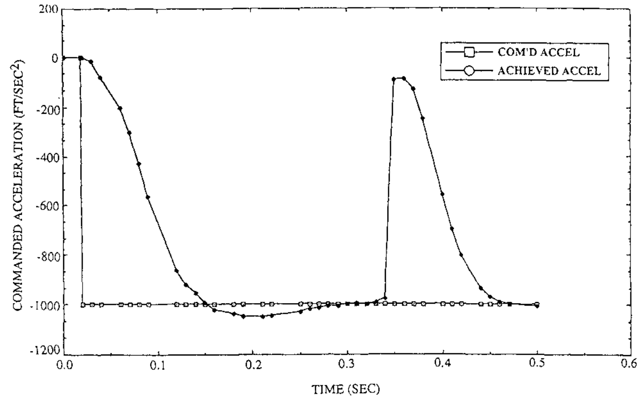

Fig. A3 Commanded and achieved lateral acceleration, with time-varying correction terms.

Now, apply the feedback linearization technique. Let

$$Z_1 = a \tag{A11}$$

$$Z_2 = \dot{Z}_1 = \dot{Z}'_\alpha \alpha + Z'_\alpha (q - \dot{\gamma}) \tag{A12}$$

$$\dot{Z}_2 = \dot{Z}'_\alpha \dot{\alpha} + \ddot{Z}'_\alpha \alpha + \dot{Z}'_\alpha (q - \dot{\gamma}) + Z'_\alpha (\dot{q} - N'_\alpha \dot{\alpha} - \dot{N}'_\alpha \alpha) \tag{A13}$$

Making appropriate substitutions for α and $\dot{\gamma}$ provides the final, transformed system

$$\dot{Z}_1 = Z_2 \tag{A14}$$

$$\dot{Z}_2 = 2\dot{Z}'_\alpha [q + (a/V_M)] + \ddot{Z}'_\alpha \alpha$$
$$+ Z'_\alpha [M_\alpha \alpha + M_\delta \delta - N'_\alpha [q + (a/V_M)] - \dot{N}'_\alpha \alpha] \equiv V \tag{A15}$$

First consider the output/input relationship from V to Z_1. Define V as

$$V = A \int (V_c - Z_1)\,\mathrm{d}t - B \int Z_2\,\mathrm{d}t - C \int Z_1\,\mathrm{d}t - DZ_2 - EZ_1 \tag{A16}$$

and substitute into Eqs. (A14) and (A15). This results in the set of equations

$$sZ_1 - Z_2 = 0 \tag{A17}$$

$$\left[\frac{(A+C)}{s} + E\right] Z_1 + \left(\frac{B}{s} + D + s\right) Z_2 = \frac{AV_c}{s} \tag{A18}$$

which can be simply solved to give

$$\frac{Z_1}{V_c} = \frac{a}{a_c} = \frac{A}{s^3 + Ds^2 + (B+E)s + (A+C)} \tag{A19}$$

This is identical to the form of Eq. (A1) if $B = 0$.

Consider Eq. (A1) again and note the following equivalences (with $B = 0$):

$$A = KK_I V_M N \tag{A20}$$

$$C = K_I N \tag{A21}$$

$$D = N_\alpha + K_q M_\delta \tag{A22}$$

$$E = -M_\alpha + K_q N = K_I M_\delta \tag{A23}$$

There are four constants (A, C, D, and E), but only three gains (K, K_I, and K_q). Thus, for example, one can obtain D by choosing K_q, E by choosing K_I with K_q given, and A by choosing K with K_q and K_I given. However, C is not specified and can vary as K_I and N vary.

Consider now the feedback linearization technique with the constraints $B = C = 0$. This will ensure a transfer function of the form [from Eq. (A19)]

$$\frac{a}{a_c} = \frac{A}{s^3 + Ds^2 + Es + A} \Rightarrow \text{D.C. gain} = 1 \tag{A24}$$

and V, given by Eq. (A16) becomes

$$V = A \int (V_c - Z_1)\,\mathrm{d}t - DZ_2 - EZ_1 \tag{A25}$$

From Eqs. (A14) and (A15), with V given by Eq. (A25) and A, D, and E given by Eqs. (A20), (A22), and (A23), respectively, the δ required to insure a linear, time-invariant transfer function for a/a_c is found to be

$$\delta = \frac{1}{Z'_\alpha M_\delta} \left[\begin{array}{c} (-Z'_\alpha M_\alpha \alpha) + (Z'_\alpha N'_\alpha - 2\dot{Z}'_\alpha)\left(q + \dfrac{a}{V}\right) \\ -\ddot{Z}'_\alpha \alpha + Z'_\alpha \dot{N}'_\alpha \alpha + KK_I V_M N \displaystyle\int (a - a_c)\,\mathrm{d}t \\ -(N'_\alpha + K_q M_\delta)\left[\dot{Z}'_\alpha \alpha + Z'_\alpha\left(q + \dfrac{a}{V}\right)\right] \\ -(-M_\alpha + K_q N + K_I M_\delta) Z'_\alpha \left(\theta + \displaystyle\int \dfrac{a}{V}\,\mathrm{d}t\right) \end{array} \right] \tag{A26}$$

Simplifying and reducing Eq. (A26) (recall that $Z'_\alpha M_\delta = -V_M N$) yields

$$\delta = KK_I \int (a_c - a)\,\mathrm{d}t + K_I(\gamma - \theta) - K_q q + (CR) \tag{A27}$$

where (CR) represents the time-varying terms.

Except for the time-varying terms and the $K_I \gamma$ term, which are apparently required for linear time invariance, Eq. (A27) is the three-loop autopilot structure. Making one further substitution into Eq. (A27), i.e., $\gamma - \theta = -\alpha$, yields

$$\delta = KK_I \int (a_c - a)\,\mathrm{d}t - K_I \alpha - K_q q + (CR) \tag{A28}$$

which is the identical format and structure of the $\dot{\gamma}$ autopilot developed using feedback linearization. This indicates that the feedback of $\dot{\theta}$ alone through the integrator is insufficient in the middle loop of the three-loop autopilot. These results are characterized in Figs. A2 and A3, which depict commanded and attained lateral accelerations from 6-DOF digital simulation runs for a case where the corrections are not included and a case where they are included.

We have thus shown the following: 1) in order to generate a linear time-invariant input-output map, the use of α feedback in lieu of $\int \dot{\theta}\,\mathrm{d}t$ is dictated for the middle loop in the three-loop autopilot configuration; 2) compensation for the rapid variations in N'_α

(i.e., $\dot{N}'_\alpha$ and $\ddot{N}'_\alpha$) is performed via the feedback terms incorporated in the CR factor.

References

[1]Li, W., and Slotine, J. E., *Applied Nonlinear Control*, Prentice–Hall, Englewood Cliffs, NJ, 1991, pp. 207–275.

[2]Nijmeijer, H., and van der Schaft, A. J., *Nonlinear Dynamical Control Systems*, Springer–Verlag, New York, 1990.

[3]Spong, M. W., and Vidyasager, M., *Robot Dynamics and Control*, Wiley, New York, 1989, pp. 259–283.

[4]Gratt, H. J., and Smith, D., "Guidance and Control Design for Advanced Kinetic Energy Missile (ADKEM)," Nichols Research Corp. Final Rept. NRC-TR-90-167, Huntsville, AL, July 1990.

[5]Tahk, M., Briggs, M. M., and Menon, P. K. A., "Applications of Plant Inversion via State Feedback to Missile Autopilot Design," *Proceedings of the 27th Conference on Decision and Control* (Austin, TX), Inst. of Electrical and Electronics Engineers, New York, 1988, pp. 730–735.

[6]Buffington, J. M., Adams, R. J., and Banda, S. S., "Robust, Nonlinear, High Angle-of-Attack Control Design for a Supermaneuverable Vehicle," *Proceedings of the 1993 Guidance, Navigation, and Control Conference* (Monterey, CA), AIAA, Washington, DC, 1993, pp. 690–700 (AIAA Paper 93-3774).

[7]Menon, P. K. A., "Nonlinear Command Augmentation System for a High Performance Aircraft," *Proceedings of the 1993 Guidance, Navigation, and Control Conference* (Monterey, CA), AIAA, Washington, DC, 1993, pp. 720–730 (AIAA Paper 93-3777).

[8]Ha, I., and Chong, S., "Design of a CLOS Guidance Law Via Feedback Linearization," *IEEE Transactions on Aerospace and Electronic Systems*, Vol. 28, No. 1, 1992, pp. 51–62.

[9]Snell, S. A., et al., "Nonlinear Inversion Flight Control for a Supermaneuverable Aircraft," *Journal of Guidance, Control, and Dynamics*, Vol. 15, No. 4, 1992, pp. 976–984.

[10]Chin, S. S., *Missile Configuration Design*, McGraw–Hill, New York, 1961, pp. 132–148.

[11]Nesline, F. W., and Nesline, M. L., "Homing Missile Autopilot Response Sensitivity to Stability Derivative Variations," *Proceedings of the 23rd Conference on Decision and Control* (Las Vegas, NV), Inst. of Electrical and Electronics Engineers, New York, 1984, pp. 1116–1121.